PB 161556

NBS

Technical Note 55

INVESTIGATION OF BEARING CREEP OF TWO FORGED ALUMINUM ALLOYS

U. S. DEPARTMENT OF COMMERCE
NATIONAL BUREAU OF STANDARDS

THE NATIONAL BUREAU OF STANDARDS

Functions and Activities

The functions of the National Bureau of Standards are set forth in the Act of Congress, March 3, 1901, as amended by Congress in Public Law 619, 1950. These include the development and maintenance of the national standards of measurement and the provision of means and methods for making measurements consistent with these standards; the determination of physical constants and properties of materials; the development of methods and instruments for testing materials, devices, and structures; advisory services to government agencies on scientific and technical problems; invention and development of devices to serve special needs of the Government; and the development of standard practices, codes, and specifications. The work includes basic and applied research, development, engineering, instrumentation, testing, evaluation, calibration services, and various consultation and information services. Research projects are also performed for other government agencies when the work relates to and supplements the basic program of the Bureau or when the Bureau's unique competence is required. The scope of activities is suggested by the listing of divisions and sections on the inside of the back cover.

Publications

The results of the Bureau's work take the form of either actual equipment and devices or published papers. These papers appear either in the Bureau's own series of publications or in the journals of professional and scientific societies. The Bureau itself publishes three periodicals available from the Government Printing Office: The Journal of Research, published in four separate sections, presents complete scientific and technical papers; the Technical News Bulletin presents summary and preliminary reports on work in progress; and Basic Radio Propagation Predictions provides data for determining the best frequencies to use for radio communications throughout the world. There are also five series of nonperiodical publications: Monographs, Applied Mathematics Series, Handbooks, Miscellaneous Publications, and Technical Notes.

Information on the Bureau's publications can be found in NBS Circular 460, Publications of the National Bureau of Standards ($1.25) and its Supplement ($1.50), available from the Superintendent of Documents, Government Printing Office, Washington 25, D.C.

NATIONAL BUREAU OF STANDARDS
Technical Note

55

AUGUST 1960

INVESTIGATION OF BEARING CREEP OF TWO FORGED ALUMINUM ALLOYS

Leonard Mordfin, Nixon Halsey, Philip J. Granum

Report to
Bureau of Naval Weapons
Department of the Navy

NBS Technical Notes are designed to supplement the Bureau's regular publications program. They provide a means for making available scientific data that are of transient or limited interest. Technical Notes may be listed or referred to in the open literature. They are for sale by the Office of Technical Services, U. S. Department of Commerce, Washington 25, D. C.

DISTRIBUTED BY

UNITED STATES DEPARTMENT OF COMMERCE

OFFICE OF TECHNICAL SERVICES

WASHINGTON 25, D. C.

Price $1.00

INVESTIGATION OF BEARING CREEP OF TWO FORGED ALUMINUM ALLOYS

Leonard Mordfin, Nixon Halsey and Philip J. Granum

Fourteen bearing specimens of 7075-T6 and 2014-T6 forged aluminum alloys were tested in creep at 400° F. The 2014-T6 specimens had greater creep resistance and less ductility than the 7075-T6 specimens.

For each material the bearing creep resistance varied directly with edge distance and bolt tightness. Prior exposure of the 2014-T6 alloy to elevated temperature reduced its bearing creep resistance.

The validity of a previously proposed theory of creep in bolted joints was examined using the test data together with results from an earlier study. The theory was found to hold for 7075-T6 but not for 2014-T6.

1. INTRODUCTION

The investigation described herein is one of a series intended to obtain useful solutions to structural creep problems by the quantitative relationship of structural creep to material creep.

A limited test program was undertaken to obtain data on bearing creep deformation for 7075-T6 and 2014-T6 forged aluminum alloys. The immediate objectives were (1) to explore the general nature of bearing creep in these materials, and (2) to examine the feasibility of calculating the creep deformations in large bolted joints which are expected to fail in bearing. In connection with the latter objective, it was proposed in an earlier report (ref. 1) that:

> A joint which is expected to fail in bearing can usually be considered to creep only in bearing. The elongation of the joint, then, is the same as that for a simple bearing specimen having the same edge distance and subjected to the same stress and temperature as the joint.

The creep deformations obtained with the bearing specimens tested in this investigation are compared with the creep deformations obtained with 7075-T6 and 2014-T6 bolted joints (fig. 1) tested in a previous study. The details of the bolted joint tests are reported elsewhere (ref. 2), but are summarized, for convenience, in Appendix A.

This report describes the material bearing creep test program and the results obtained. This investigation was conducted at the National Bureau of Standards under the sponsorship and with the financial assistance of the Bureau of Naval Weapons. The authors acknowledge the assistance of Mr. Thomas D. Field, Jr. in the design of some of the test apparatus.

2. SPECIMENS

The bearing specimens tested in this investigation were cut from the bolted joints described above and in Appendix A. They were machined from parts of the straps which had been subjected to relatively little heating. It is estimated that those portions of the straps from which the bearing specimens were taken had not been heated above 200° F and had not been stressed beyond the elastic limit corresponding to this temperature. Hence the bearing specimens did not have any prior work hardening, but undoubtedly did have a small amount of overaging because of the exposure to elevated temperature.

Two general designs of bearing specimens were tested. These are designated as "straight" and "beveled", and are shown in figs. 2 and 3. The beveled specimen is an attempt to reproduce the complex edge condition of the bolted joint specimens.

3. TEST TECHNIQUES

3.1 Loading

The tests were conducted in a 100,000 lb capacity universal screw-power testing machine, which was adapted for creep testing by the installation of a load-maintaining system similar to that described in ref. 4.

Referring to figs. 4 and 5, the specimen A was held by two steel plates B which were mounted in the upper grip of the machine and separated by a spacer plate (not shown). The bearing load was applied with a hardened steel pin C which was machined to provide a close sliding fit in the

bearing hole. The pin was held by two steel plates D which were mounted in the lower grip of the testing machine and separated by a spacer plate (not shown).

The ends of the loading pin were threaded to accommodate nuts E. These could be tightened to simulate bolt tightness in a joint. "Full" tightness could be imposed by inserting washers F and drawing the nuts up tight with a wrench. A condition of "no" tightness could be effected by removing some of the washers and leaving the nuts loose.

3.2 Deformation Measurement

Bearing deformation manifested itself primarily as an elongation of the bearing hole. This deformation was measured in terms of the displacement of the axis of the loading pin from the axis of the original hole.

A concentric rod and tube arrangement was used to transfer the displacement to the outside of the test furnace. Referring to figs. 4 and 5, tubes G were mounted parallel to each edge of the specimen. The upper ends of these were fixed on the original horizontal center line of the hole by set screws H. A rod inside each tube was attached to a yoke device which included plates J. These plates had holes drilled in them so that they fitted closely over the loading pin.

Displacement of the pin relative to the original bearing hole was thus converted into a differential movement within each of the two rod and tube assemblies. This movement was measured with a pair of differential transformers mounted on the lower ends of the rods and tubes below

the test furnace. Strip chart recorders were used to obtain records of displacement vs. time. The bearing deformation of the specimen was taken as the average of the two records.

3.3 Heating

The test furnace was fabricated from transite sheet and contained eight quartz infrared lamps. Four thermocouples were peened into the surface of each specimen. The voltages to the lamps were controlled by autotransformers. These were adjusted manually to minimize temperature gradients. Power was controlled by a time-proportioning automatic temperature controller.

Temperatures were maintained constant and uniform within 2° F during each test.

3.4 Testing Procedure

After heating the specimen to the test temperature, it was permitted to remain at that temperature for a predetermined exposure period. The test load was then applied, and this was considered time zero. Deformations were measured starting at the time that the full test load was reached. In this manner, displacements due to elastic extension, thermal expansion and backlash in the extensometer arrangement, were eliminated.

4. NOMENCLATURE

4.1 Symbols

D	diameter of loading pin, in.
e	base of natural logarithms, 2.718 ...
f_1, f_3	functions of t_x
f_2	function of t_{10}
F	test load, lb
h	thickness of bearing specimen, in.
k	characteristic dimension of beveled specimen (see fig. 3), in.
m	edge distance, in. or dimensionless (see Section 4.2)
m_{eff}	effective edge distance, in. or dimensionless (see Section 4.2)
P	a parameter defined by eq. (2)
P'	a parameter defined by eq. (4)
R	bolt tightness (see Section 4.2)
t_x	prior exposure time, hr (see Section 4.2)
t_{10}	test time to reach 0.10 in. of creep extension, hr
σ	bearing stress as defined by eq. (1), or bearing creep strength, $lb/in.^2$
σ'	bearing creep strength for $t_x = 0$, $lb/in.^2$

4.2 Definitions

Bearing stress, σ, is the compressive stress produced on the edge of the bearing hole by the loading pin. For most design purposes this

stress is considered to be uniformly distributed over the projected area of the edge of the hole, so that

$$\sigma = \frac{F}{Dh} \tag{1}$$

Edge distance, m, is the distance from the center of the bearing hole to the edge of a straight specimen, measured in the direction of loading (see fig. 2). Very often, edge distance is expressed dimensionlessly as the ratio of edge distance to pin diameter. In this investigation the diameter is 1 in., so the two representations are equivalent.

For a beveled specimen (fig. 3), the above definition does not apply so an effective edge distance, m_{eff}, must be used.

Prior exposure, t_x, is the length of time that a specimen is subjected to the test temperature prior to the application of the test load.

Bolt tightness, R, has been assigned a numerical scale from 1 to 10 where 1 represents no tightness and 10 represents full tightness.

5. TEST RESULTS FOR 7075-T6 SPECIMENS AND DISCUSSION

5.1 Straight Bearing Specimens

Five straight specimens (fig. 2) of 7075-T6 aluminum alloy were tested at 403° F to explore, in a cursory manner, the effects of bearing stress, edge distance and bolt tightness on bearing creep deformation. These tests were all conducted with a prior exposure to test temperature of 1.7 hr. The test conditions are listed:

Specimen No.	m in.	R	σ lb/in.^{2}	t_{10} hr
4	2.00	1	35,000	1.1
5	2.62	1	35,000	7.1
6	1.85	1	30,800	10.5
7	1.85	10	35,000	3.4
8	1.85	10	35,000	3.3

The creep deformation curves are given in fig. 6. These were condensed from the continuous strip chart records. The curves do not exhibit a conventional steady-state creep stage, nor do they plot as straight lines on log paper. Hence, neither steady-state creep rates nor simple power functions could be used to characterize the curves. Instead, t_{10}, "the test time required to reach 0.10 in. of creep deformation", was arbitarily chosen as a simple measure of creep resistance by which the curves could be compared. Values of t_{10} are listed in the table above.

Using the data in the table, it was deduced that the relative effects of stress, edge distance and bolt tightness could be adequately described by means of the empirical parameter

$$P = Rm^{10}e^{-\sigma/1000} \tag{2}$$

This parameter was related to t_{10} with a curve-fitting process, giving the empirical equation

$$t_{10} = 10^7 eP^{0.6}. \tag{3}$$

A comparison of this equation with the experimental data is shown in fig. 7.

Neither eq. (2) nor eq. (3) has any value except for the specimens and the range of variables involved here. The equations are used in this report merely to show the relative effects of the different test variables and to facilitate interpolation of them.

Examination of eqs. (2) and (3) reveals that creep resistance decreases rapidly with increasing bearing stress. Increasing edge distance raises the creep resistance, even for values as high as 2.62. Furthermore, bolt tightness increases the creep resistance.

The strengthening effect of bolt tightness, insofar as creep is concerned, is one that has received little consideration as revealed by the literature. This effect is discussed further in the following section.

5.1.1 Effect of Bolt Tightness

Intuitively, it seems that bolt tightness improves bearing creep resistance by (1) diverting some of the nominal bearing force toward overcoming friction between the faying surfaces, (2) restraining lateral deformation in a direction parallel to the bolt axis, or (3) both.

Yerkovich, in reporting the results of creep tests on riveted joints, ref. 5, attributed the improvement in bearing creep resistance to friction between the faying surfaces.

The tests of specimens 7 and 8 were designed to investigate this effect. The conditions for these two tests were identical with one exception. The washers (F, fig. 5) for specimen 7 were steel while those for specimen 8 were aluminum. This difference was introduced to examine the effect of friction between the washers and the specimen. The coefficient of sliding friction for an aluminum/aluminum interface is about three times that for an aluminum/steel interface, ref. 6. Nevertheless, fig. 6 shows that the creep curves are virtually identical.

This suggests only one explanation: Bolt tightness improves the creep resistance of the bearing specimens by restraining lateral deformation in a direction parallel to the bolt axis. This deformation is illustrated in fig. 8. Specimens 4 and 9, fig. 8, are both 7075-T6 aluminum alloy; specimen 4 was tested with no bolt tightness while specimen 9 had full bolt tightness. In the former case considerable lateral deformation is apparent; in the latter case, comparatively little.

As a result of this effect, the proposition presented on page 2 must be broadened. Specifically, the word "stress" should be interpreted to include lateral restraint as well as nominal bearing stress.

5.2 Beveled Bearing Specimens

Two beveled specimens of 7075-T6 aluminum alloy were tested to evaluate the effective edge distance for this design. Both tests were conducted at 403° F following a prior exposure of 1.7 hr, with a nominal bearing stress of 35,000 lb/in.^{2} and full bolt tightness. The dimensions k (fig. 3) and the test results obtained were:

Specimen	$\frac{k}{\text{in.}}$	$\frac{t_{10}}{\text{hr}}$
9	2.50	3.0
10	2.62	4.6

The values of t_{10} were taken from the creep deformation records, which are reproduced in fig. 9. With these values, the parameter P for each specimen was taken from fig. 7. Then, with eq. (2), it was calculated that

$$m_{eff} = 1.83 \text{ in. for specimen 9, and}$$
$$m_{eff} = 1.96 \text{ in. for specimen 10.}$$

A comparison of these values with the dimension k reveals that $m_{eff} \approx \frac{3}{4} k$.

5.3 Bolted Joint Specimen

The 7075-T6 bolted joint specimen which was discussed in the Introduction and in Appendix A had an edge condition similar to that of specimen 10. Furthermore, it was tested under the same stress and temperature conditions as specimen 10. Hence, according to the proposition on page 2, the joint should yield the same creep curve as specimen 10. The creep curves for the joint and for the bearing specimen are given in fig. 10, from which it is apparent that some discrepancy exists between the two.

For design purposes, it is desirable to evaluate the magnitude of this discrepancy in terms of stress. From the curve for the bolted joint

it is seen that $t_{10} = 6.0$ hr. Entering fig. 7 with this value gives $P = 8.0 \times 10^{-12}$. Now, using $m_{eff} = 1.96$ in. and $R = 10$, eq. (2) shows that the effective bearing stress for the bolted joint is 34,600 lb/in.^{2} This is only 1.1 percent less than the actual bearing stress and represents a stress-wise error that is generally negligible.

6. TEST RESULTS FOR 2014-T6 SPECIMENS AND DISCUSSION

6.1 Bearing Specimens

Seven bearing specimens of 2014-T6 aluminum alloy were tested at 398° F. The test conditions are listed in the table below and the creep curves are given in fig. 11. Examination of these data reveals that the creep properties of 2014-T6 are superior to those of 7075-T6 at 400° F.

An additional test variable, prior exposure time, was introduced in this series of tests. Because of this additional variable, the parameter P, defined by eq. (2) must be modified to incorporate the effects of prior exposure as follows:

$$P' = P(1+t_x)^{-0.8} \qquad (4)$$

The exponent in this equation was determined by a curve-fitting process.

Tests of 2014-T6 Bearing Specimens

Specimen	Type[a]	m in.	k in.	R	t_x hr	σ lb/in^2	t_{10} hr
3	S	2.00	b	1	1.7	50,000	5.0
11	B	b	2.62	10	48.4	50,000	4.8
12	B	b	2.62	10	1.7	50,000	20.4
13	B	b	2.62	10	48.4	34,000	c
14	B	b	2.62	10	48.4	46,700	22.0
15	S	2.62	b	10	48.4	46,700	27.7
16	B	b	2.62	10	1.7	46,700	27.0

a. S = straight; B = beveled

b. Not applicable

c. Test discontinued at 116 hr, before reaching 0.10 in. of creep.

A plot of t_{10} vs. P' for the 2014-T6 bearing specimens is given in fig. 12. The dashed line was faired through the plotted points.

The parameter P' is empirical, and only applies to the specimens and the range of variables discussed here. It is used in this report only to indicate the relative effects of the different test variables on the creep resistance of the bearing specimens.

It may be seen that bearing stress, edge distance and bolt tightness affect the creep resistance of the 2014-T6 specimens in the same general manner in which they affected the creep resistance of the 7075-T6 specimens. Furthermore, the creep resistance of the 2014-T6 specimens is reduced by

increasing the prior exposure time. The nature of this reduction is discussed further in the following section.

6.1.1 Effect of Prior Exposure

It was postulated in ref. 2 that, for a given material at a given temperature,

$$\sigma = f_1 \sigma' \tag{5}$$

where σ is creep strength following an exposure, σ' is creep strength without a prior exposure, and f_1 is a function of the exposure time only.

Based on the data obtained in this investigation, it is shown in the Appendix that

$$\sigma = \sigma' - f_3 \tag{6}$$

where f_3 is a function of the exposure time only.

It is obvious that eqs. (5) and (6) are not compatible. In all probability, eq. (5) is incorrect, but eq. (6) should not be employed for design purposes without obtaining further experimental verification.

6.2 Bolted Joint Specimen

The 2014-T6 bolted joint specimen which was discussed in the Introduction and in Appendix A had an edge condition similar to that of specimen 11. Furthermore, it was tested under the same stress, temperature and exposure conditions as specimen 11. A comparison of the creep curves

for the bolted joint and for specimen 11 is given in fig. 13. It is clear from this figure that virtually no correlation exists between the two, indicating that the proposition on page 2 does not apply in this case.

This is not entirely unexpected, and was foreseen some time ago in ref. 7. The theory holds only for ductile materials which have the ability to rapidly relax the stress concentrations around holes by plastic flow, while still retaining considerable creep strength and ductility (ref. 8). At 400° F, however, 2014-T6 is relatively brittle in creep, and presumably does not permit the relief of stress concentrations prior to fracture. The presence of this relative brittleness is evidenced by fig. 11, which indicates small values of extension at rupture, and by fig. 8, where specimens 3 and 16 are 2014-T6 and specimens 4 and 9 are 7075-T6.

What is surprising is that the joint exhibited greater creep resistance than the corresponding bearing specimen, fig. 13. Studies of the possible effects of overaging, interaction between bolt holes in the joint, oversized holes, and multiaxiality of stress were made in an attempt to explain this apparent anomaly. However, to date the authors are unable to offer a rational explanation for this unusual behavior.

7. CONCLUSIONS

The bearing creep properties of 2014-T6 forged aluminum alloy are superior to those of 7075-T6 forged aluminum alloy at 400° F. At this

temperature, 2014-T6 exhibits considerably less ductility than 7075-T6. These conclusions corroborate similar ones obtained in ref. 2.

Based on the limited number of tests performed, it appears that the bearing creep resistance of the two alloys increases both with increased edge distance and with increased bolt tightness. The beneficial effect of bolt tightness is seemingly due to restraint of lateral deformation in a direction parallel to the bolt axis, rather than to friction. Exposure of 2014-T6 to elevated temperature for a period of time prior to loading apparently reduces the bearing creep resistance.

The creep strength of a 7075-T6 bolted joint, which had been designed to fail in bearing, was found to agree closely with the creep strength of a 7075-T6 bearing specimen under the same edge, stress and temperature conditions.

The creep resistance of a 2014-T6 bolted joint was considerably greater than that of a comparable bearing specimen.

8. REFERENCES

1. L. Mordfin and A. C. Legate, "Creep Behavior of Structural Joints of Aircraft Materials Under Constant Loads and Temperatures", NACA TN 3842, 1957.

2. L. Mordfin, G. E. Greene, N. Halsey, R. H. Harwell, Jr., and R. L. Bloss, "Creep and Static Strengths of Large Bolted Joints of Forged Aluminum Alloys Under Various Temperature Conditions", NBS Rep. 5442 on BuAer Project TED NBS AD-222, July 1957, unpublished; also IAS Paper 779, 1958.

3. L. Mordfin, "Creep and Creep-Rupture Characteristics of Some Riveted and Spot-Welded Lap Joints of Aircraft Materials", NACA TN 3412, 1955.

4. A. H. Stang and L. R. Sweetman, "Speed Control for Screw-Power Testing Machines Driven by Direct-Current Motors", ASTM Bul. No. 87, Aug. 1937.

5. L. A. Yerkovich, "Investigation of the Compressive, Bearing, and Shear Creep-Rupture Properties of Aircraft Structural Metals and Joints at Elevated Temperatures", WADC TR 54-270, Part IV, May 1958.

6. T. Baumeister (ed.), "Marks' Mechanical Engineers' Handbook", McGraw-Hill Book Co., New York, N. Y., 6th ed., 1958, p. 3-40.

7. L. Mordfin, "The Creep of Structural Joints", Proc. Fla. Conf. on High-Speed Aerodynamics and Structures, ARDC TR 57-46, vol. 1, 1957.

8. L. Mordfin, N. Halsey and G. E. Greene, "Effects of Concentration and Interaction of Stresses on Tensile Rupture Strength of Riveted Joints", Appendix A to "Investigations of Creep Behavior of Structural Joints Under Cyclic Loads and Temperatures", NASA TN D-181, 1959.

APPENDIX A

SUMMARY OF PERTINENT INFORMATION FROM REF. 2

Bolted joints, fig. 1, were fabricated from forged aluminum alloy slabs and high strength steel bolts. They were creep tested under constant loads and temperatures following an unloaded exposure to the test temperature. The test conditions were as follows:

Joint material	Prior exposure hr	Temperature °F	Bearing stress lb/in^2
7075-T6*	1.7	403	35,000
2014-T6*	48.4	398	50,000

The 7075-T6 joint exhibited considerably more ductility than the 2014-T6 joint. By using the joint efficiencies in the manner described in ref. 3, the failure times were calculated from the tensile rupture properties of the materials. Agreement between the calculated and the actual failure times was satisfactory, as shown:

Joint	Actual failure hr	Calculated failure hr
7075-T6	9.6	8.7
2014-T6	31.	25.

---

*In ref. 2 these joints were designated as 7075-T6-3 and 2014-T6-3, respectively.

APPENDIX B

DERIVATION OF EQUATION (6)

Substituting eq. (2) into eq. (4) and solving for σ gives

$$\sigma = 1000\,[\log(Rm^{10}) - 0.8\,\log(1+t_x) - \log P'] \qquad (7)$$

From fig. 12 it is seen that P' is a function of t_{10}. Hence

$$\sigma = 1000\,[\log(Rm^{10}) - 0.8\,\log(1+t_x) - f_2(t_{10})] \qquad (8)$$

When $t_x = 0$, the creep strength reduces to

$$\sigma' = 1000\,[\log(Rm^{10}) - f_2(t_{10})] \qquad (9)$$

Substituting eq. (9) into eq. (8),

$$\sigma = \sigma' - 800\,\log(1+t_x) \qquad (10)$$

or,

$$\sigma = \sigma' - f_3 \qquad (6)$$

where f_3 is a function of the exposure time.

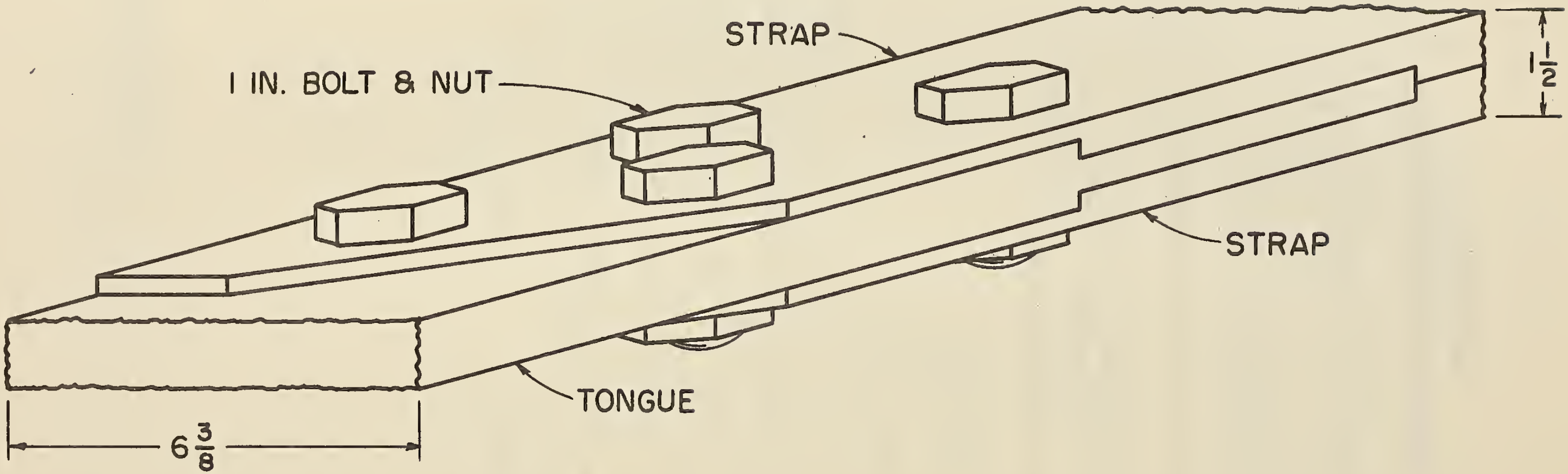

Fig. 1 BOLTED JOINT SPECIMEN

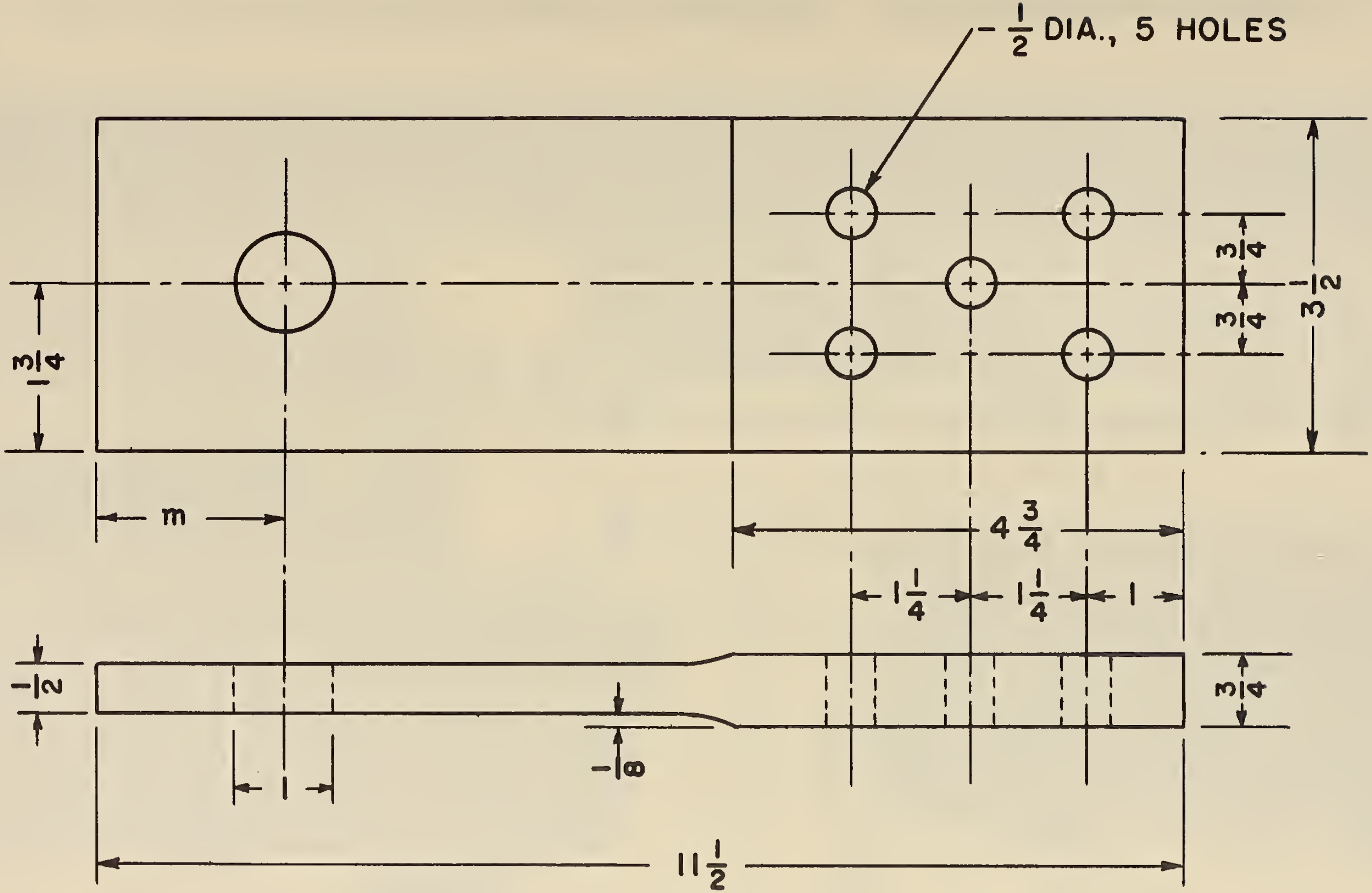

Fig. 2 Details of straight bearing specimen. All dimensions in inches.

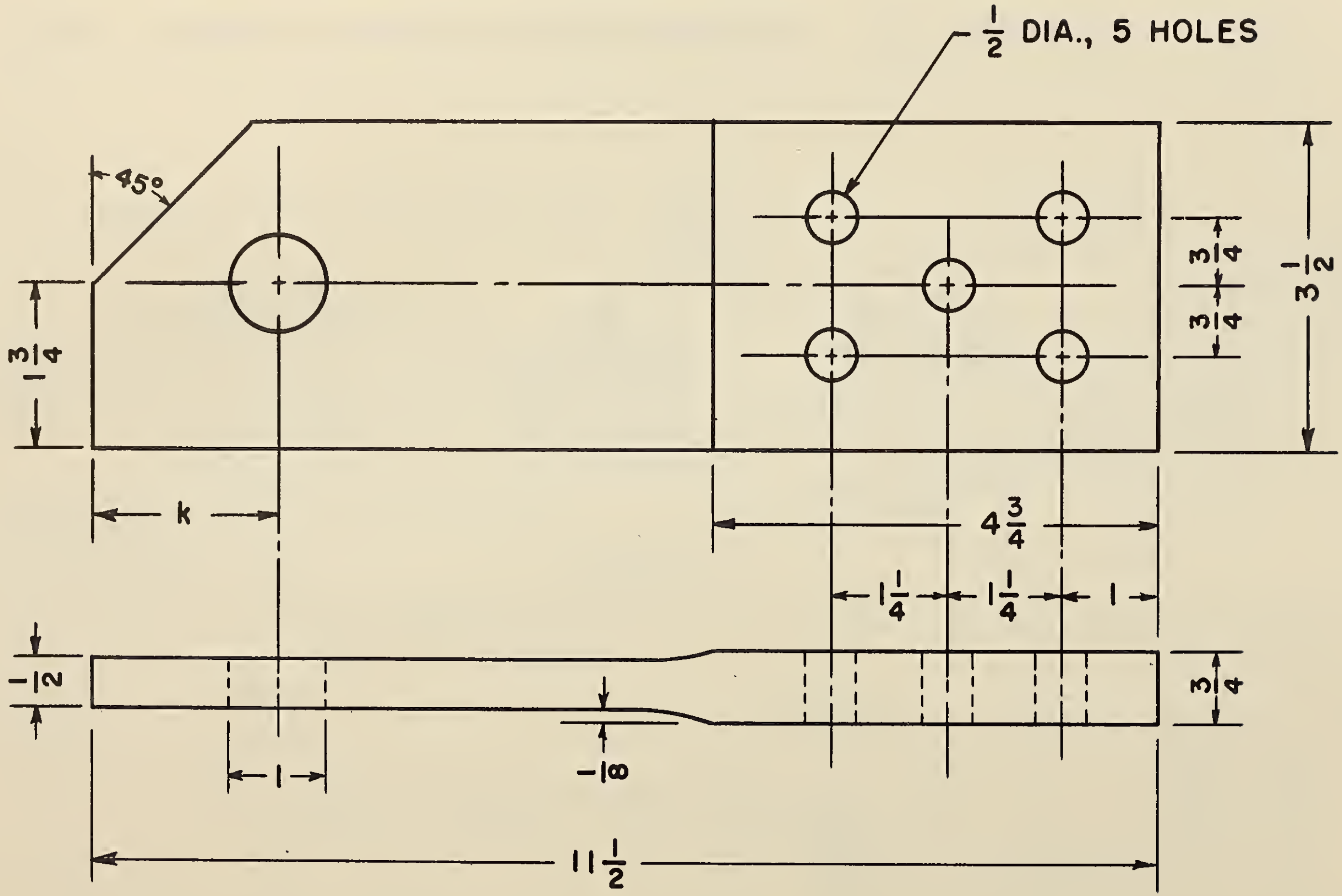

Fig. 3 Details of beveled bearing specimen. All dimensions in inches.

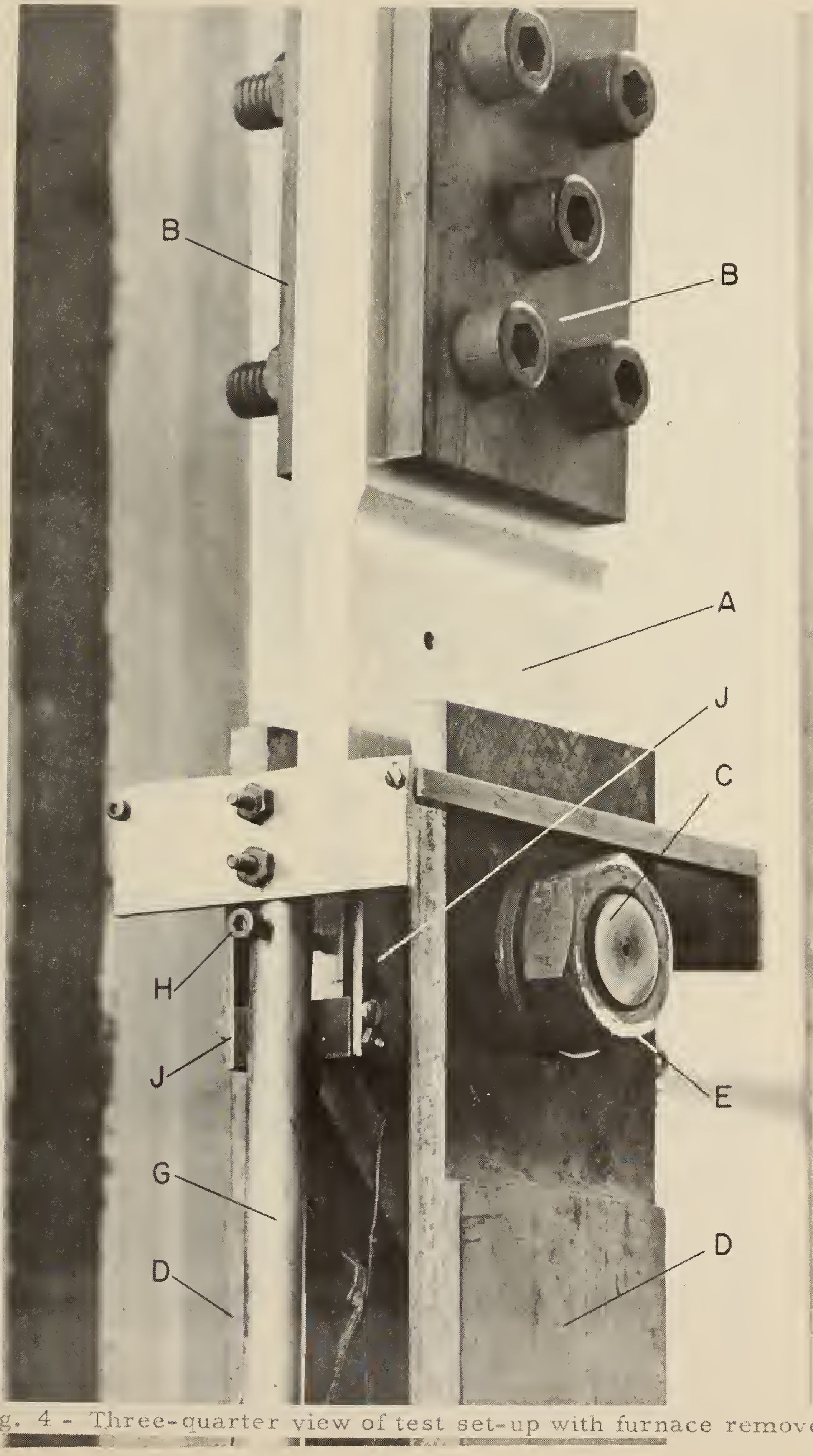

Fig. 4 - Three-quarter view of test set-up with furnace removed.

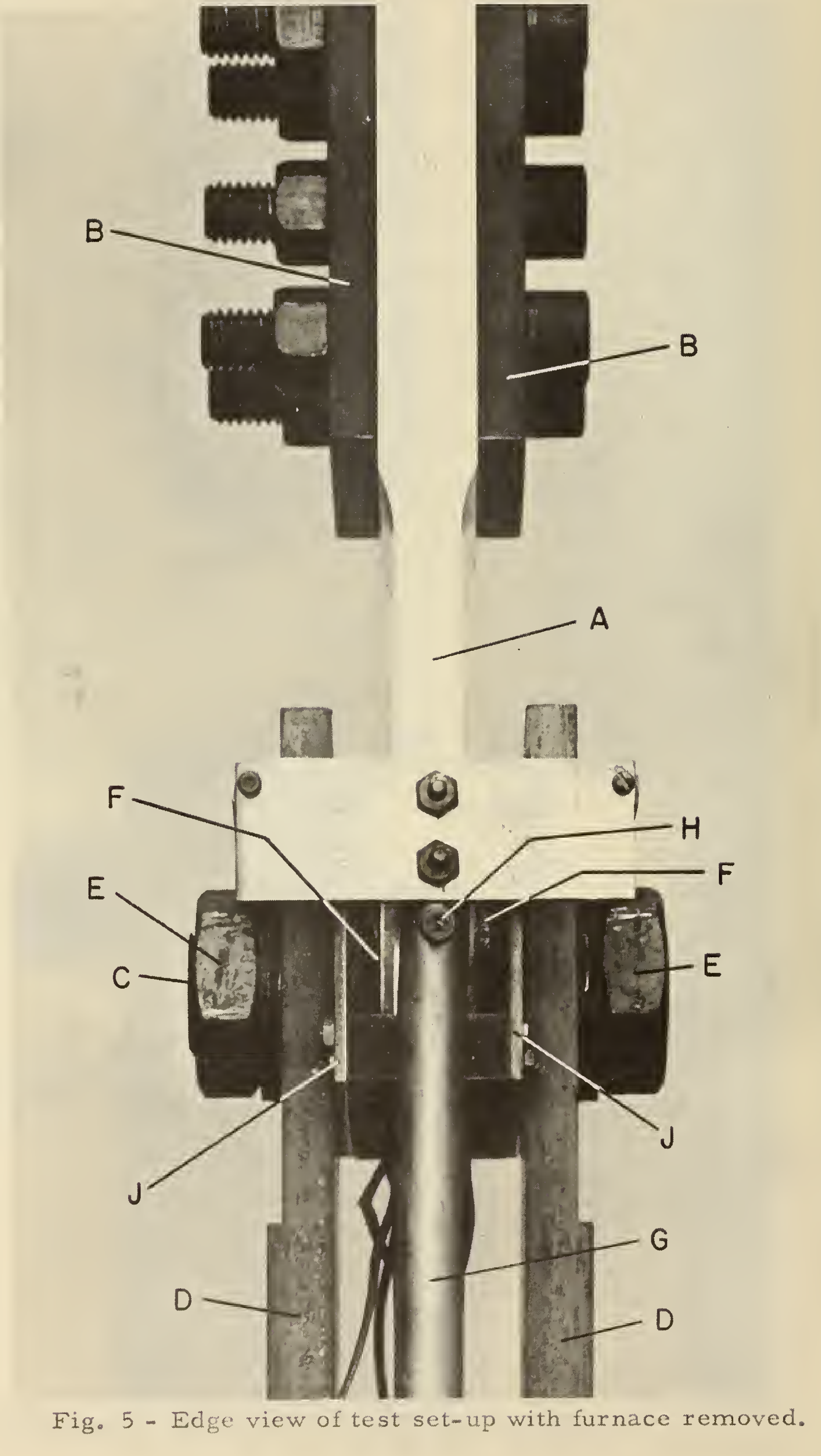

Fig. 5 - Edge view of test set-up with furnace removed.

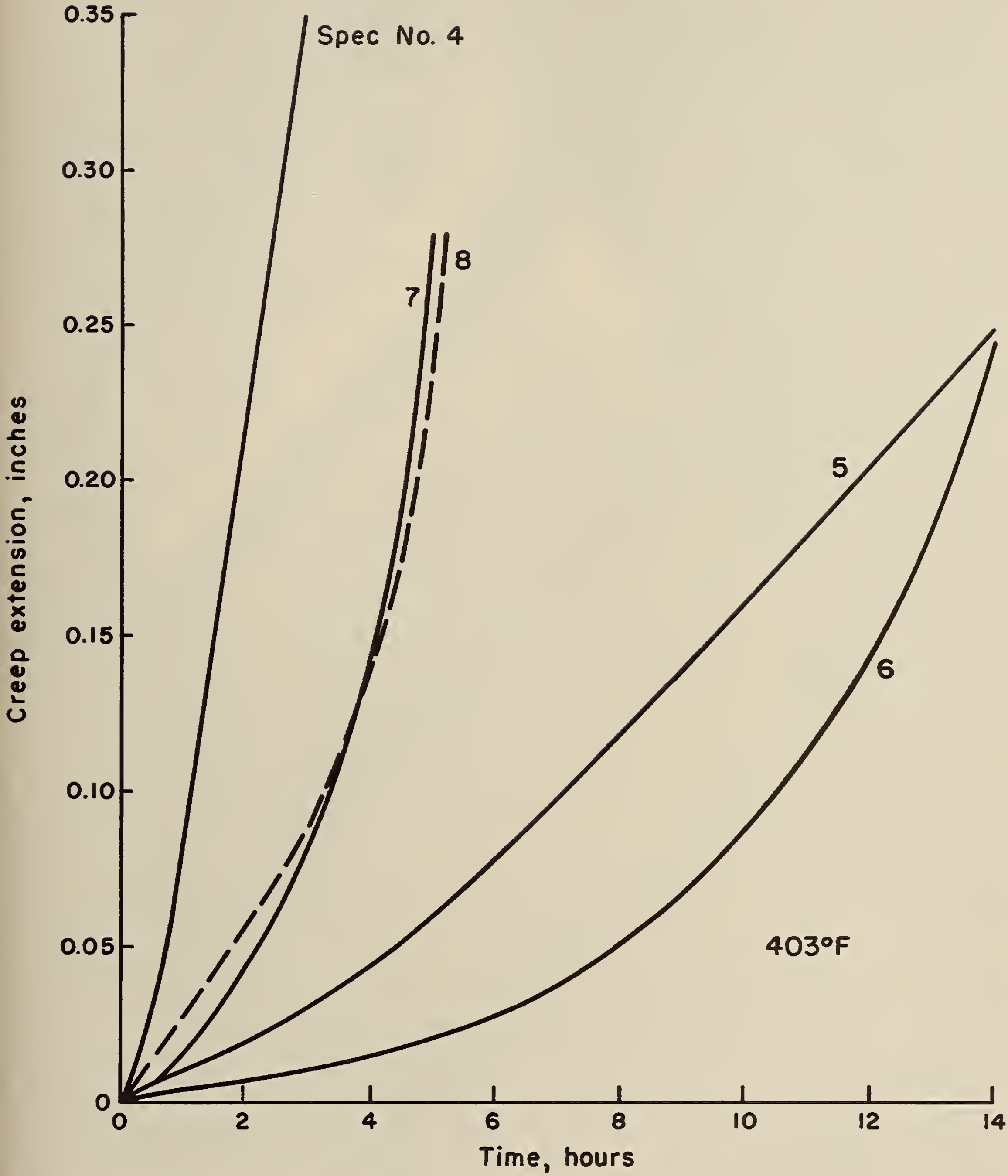

Fig. 6 Bearing creep curves of 7075-T6 straight specimens.

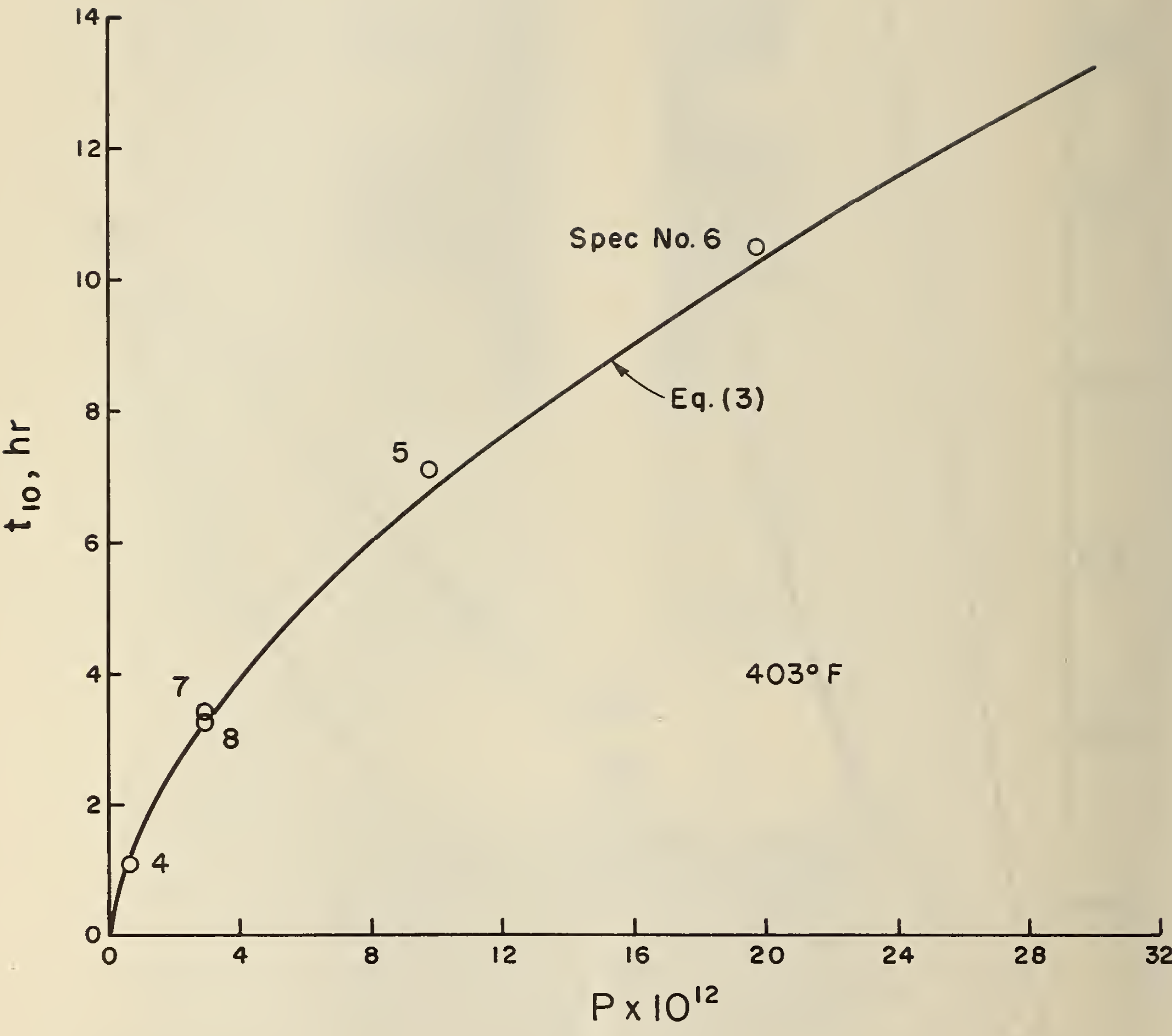

Fig. 7 Creep resistance of 7075-T6 straight specimens in parametric form.

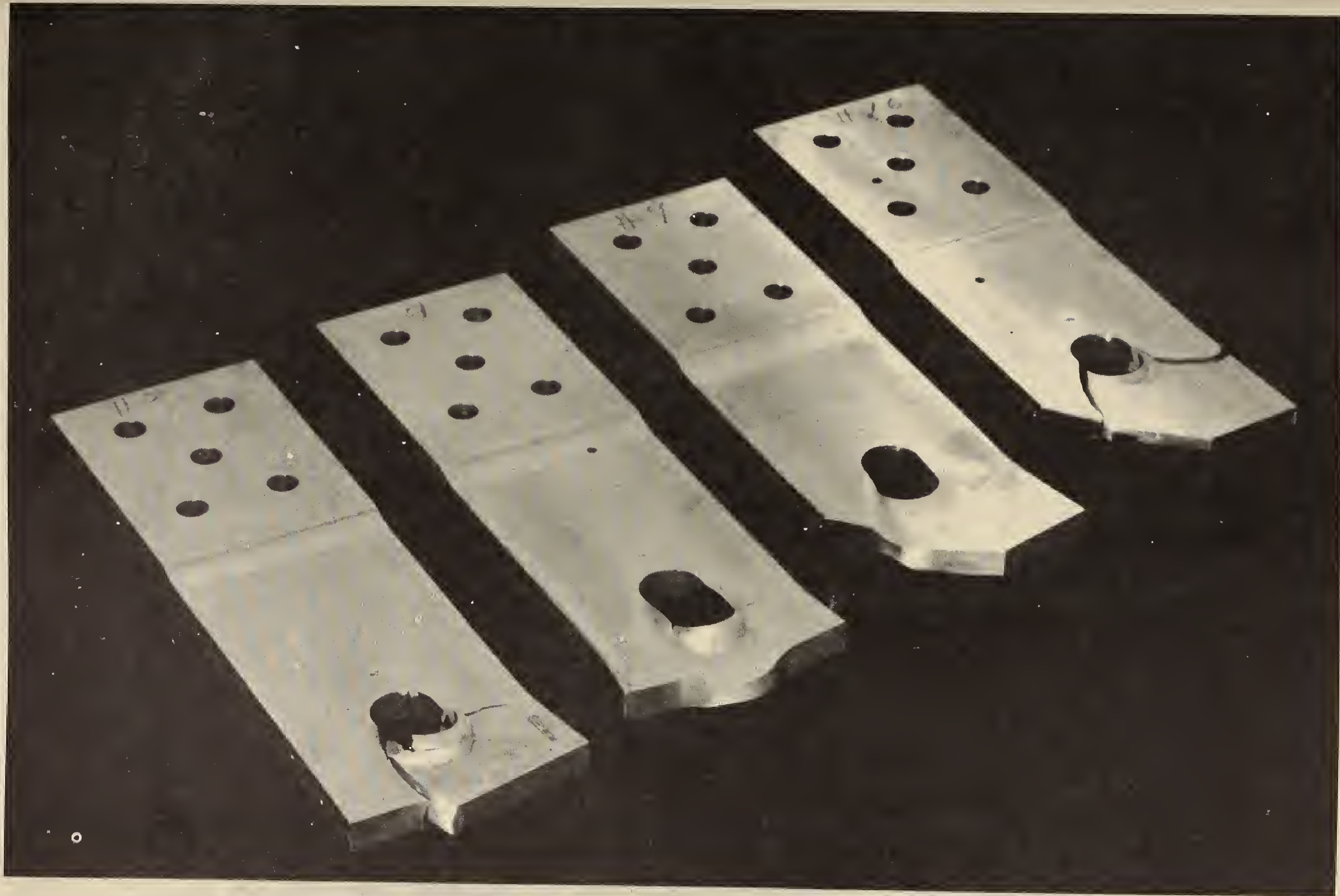

Fig. 8 - Bearing creep specimens after testing. Left to right: specimens 3, 4, 9 and 16.

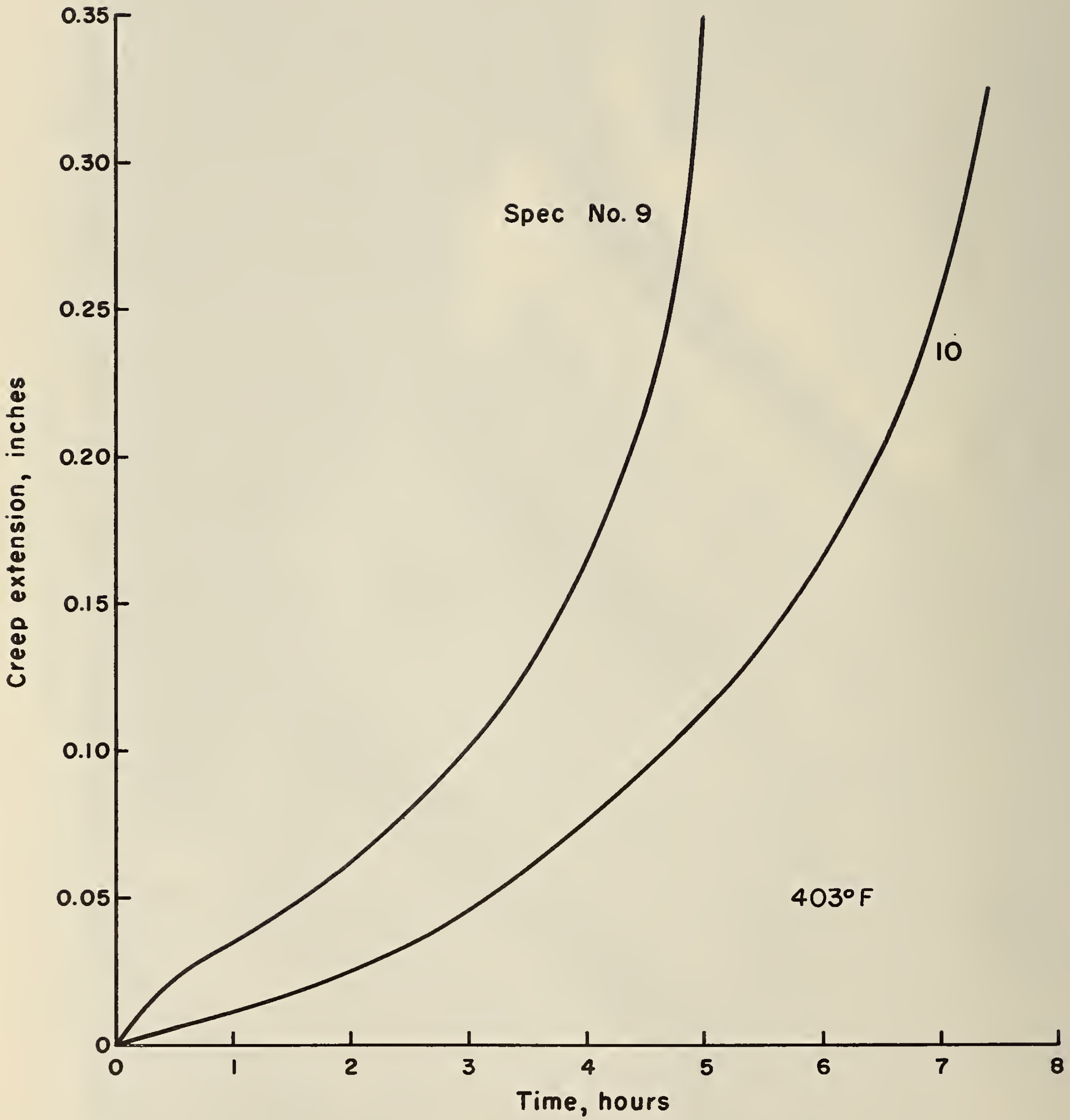

Fig. 9 Bearing creep curves of 7075-T6 beveled specimens.

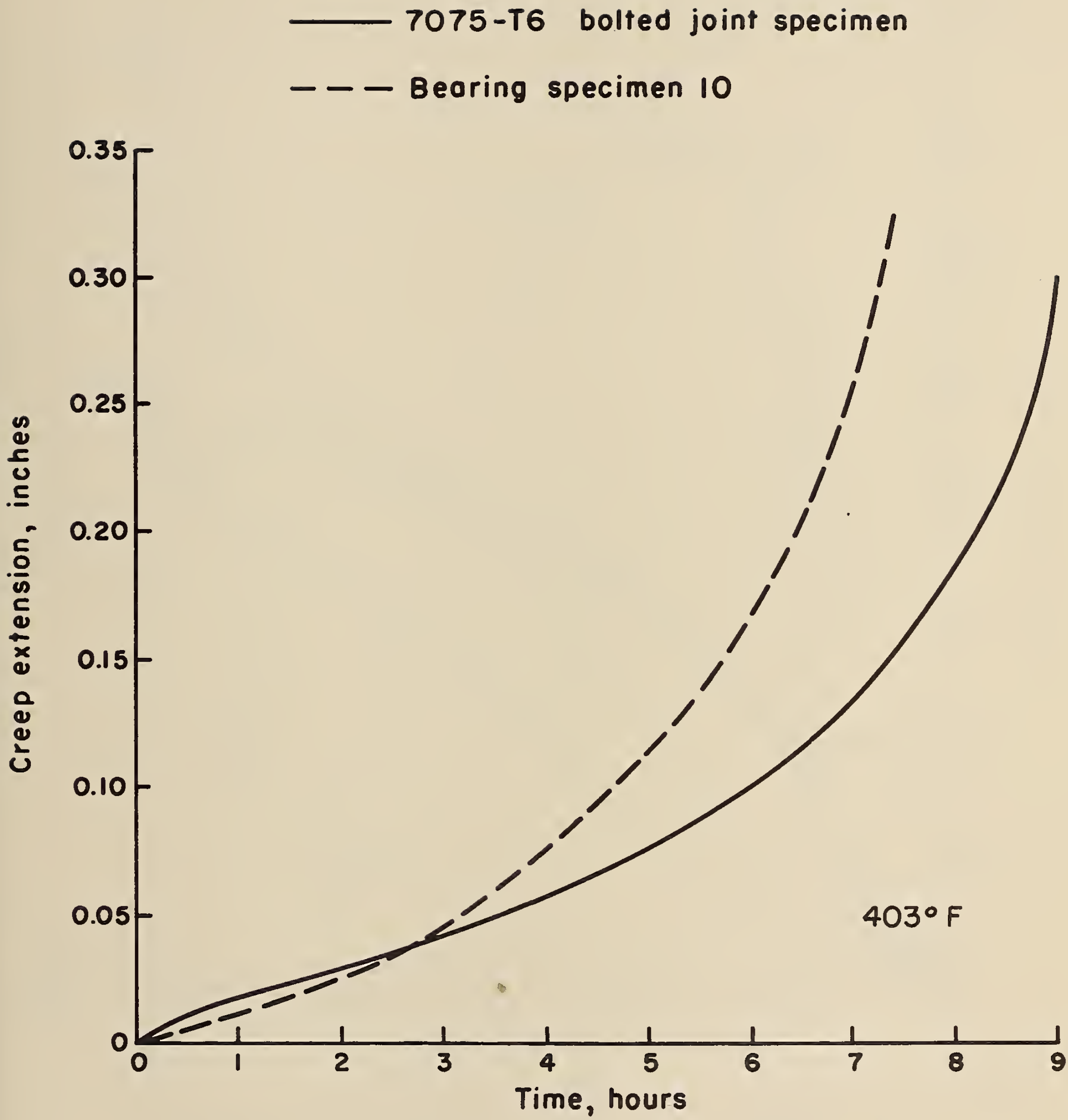

Fig. 10 Comparison of creep curves for 7075-T6 bolted joint and bearing specimen 10.

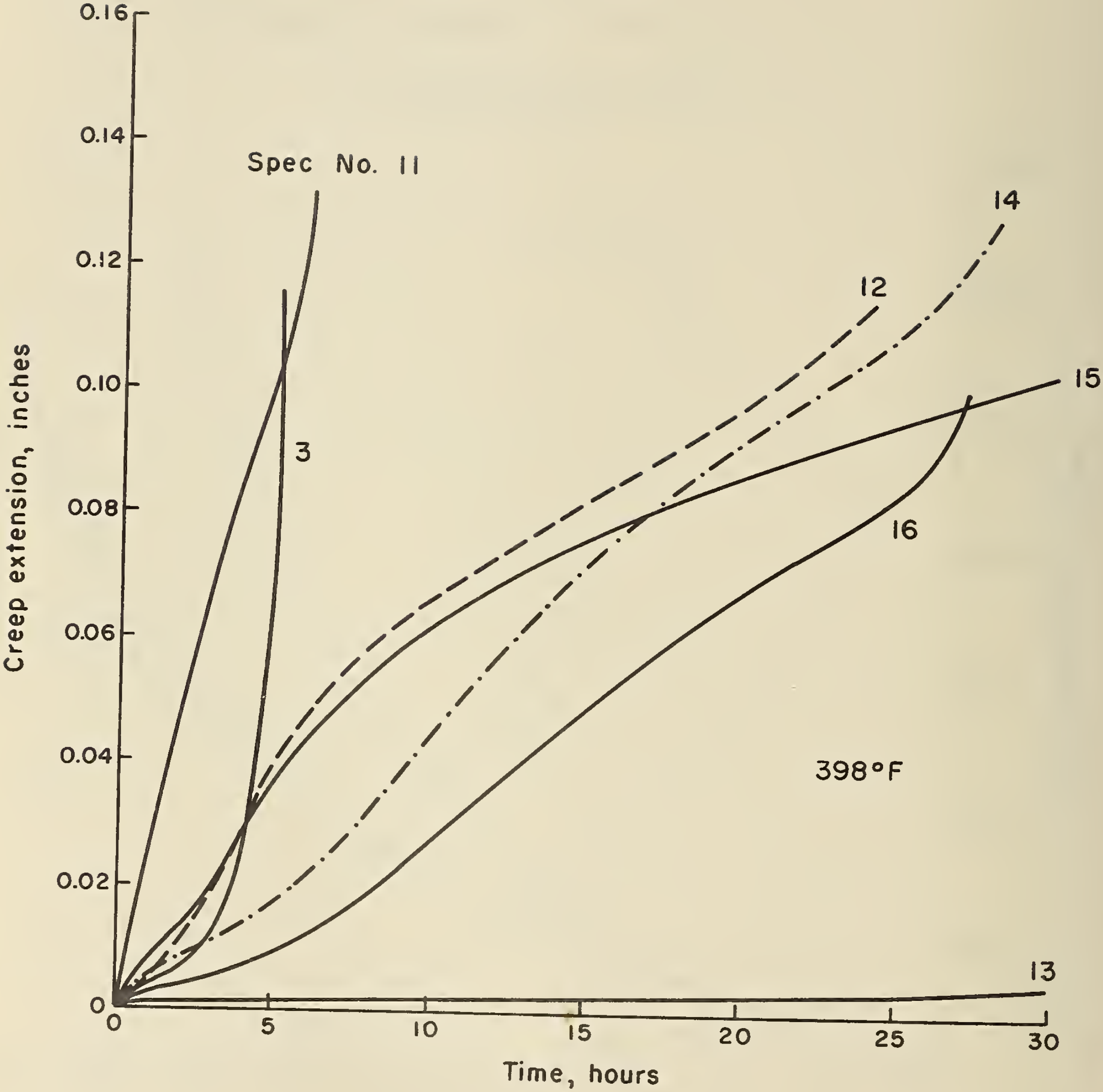

Fig. 11 Bearing creep curves for 2014-T6 specimens

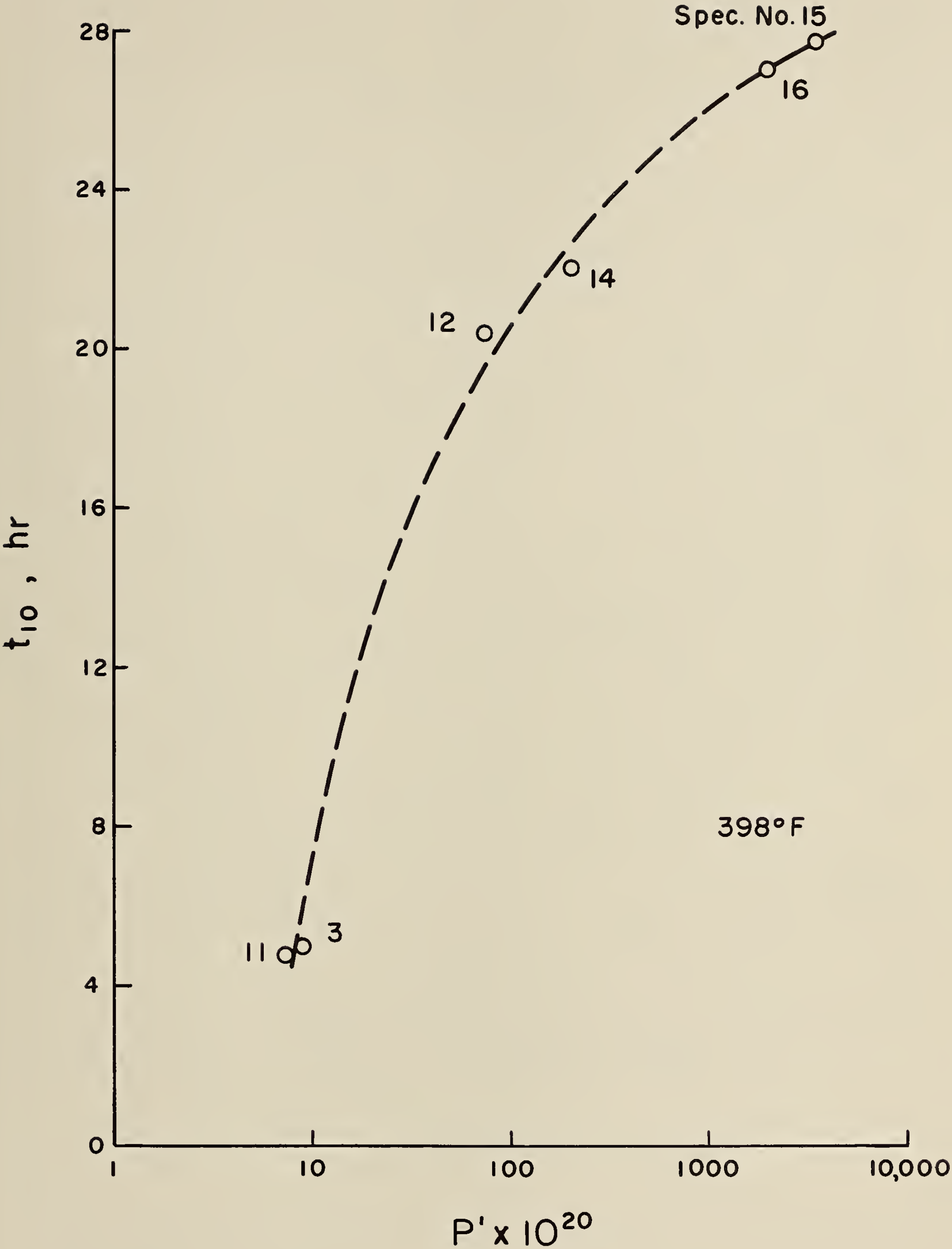

Fig. 12 Creep resistance of 2014-T6 specimens in parametric form.

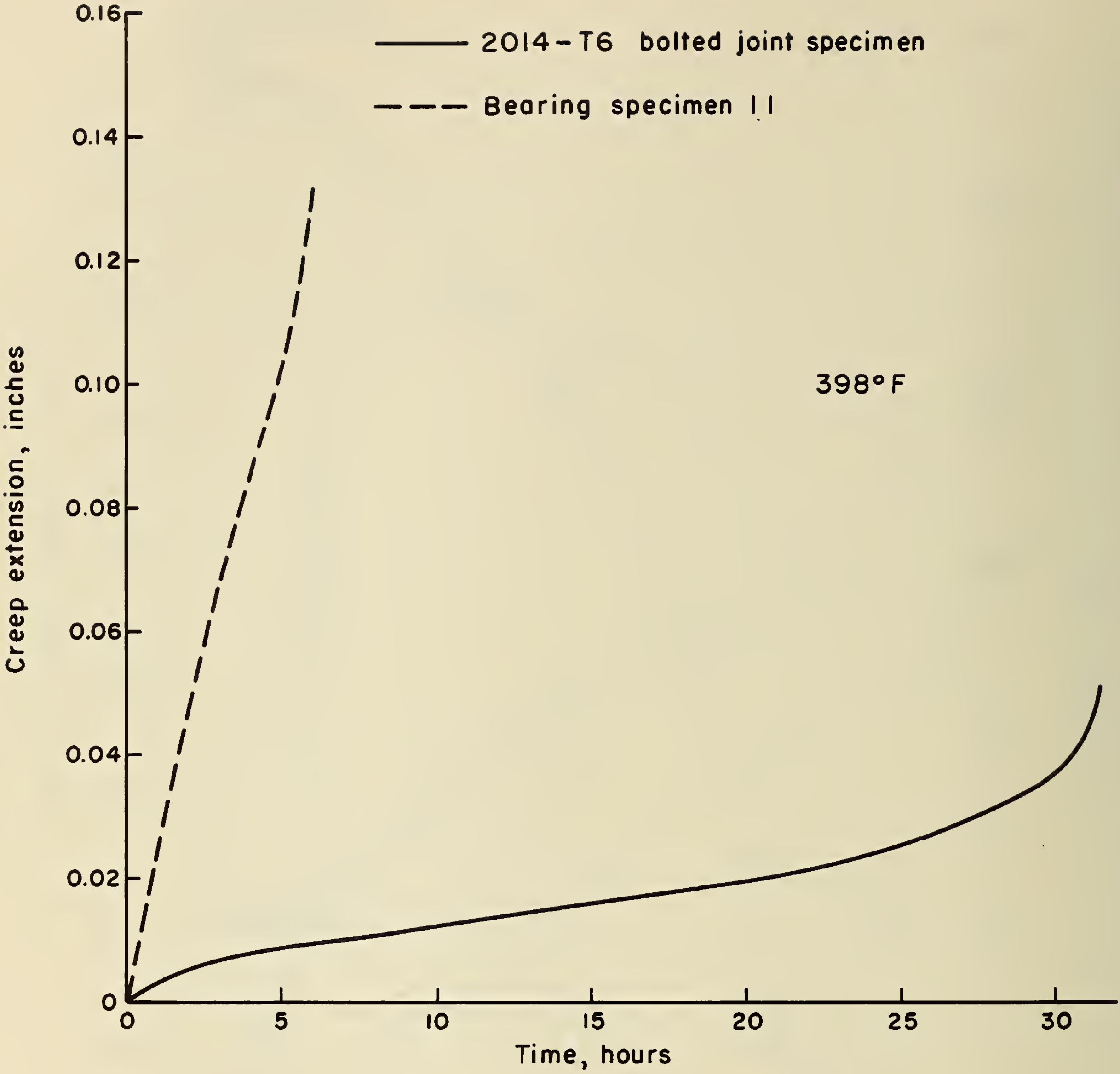

Fig. 13 Comparison of creep curves for 2014-T6 bolted joint and bearing specimen 11.

U.S. DEPARTMENT OF COMMERCE
Frederick H. Mueller, *Secretary*

NATIONAL BUREAU OF STANDARDS
A. V. Astin, *Director*

THE NATIONAL BUREAU OF STANDARDS

The scope of activities of the National Bureau of Standards at its major laboratories in Washington, D.C., and Boulder, Colorado, is suggested in the following listing of the divisions and sections engaged in technical work. In general, each section carries out specialized research, development, and engineering in the field indicated by its title. A brief description of the activities, and of the resultant publications, appears on the inside of the front cover.

WASHINGTON, D.C.

Electricity and Electronics. Resistance and Reactance. Electron Devices. Electrical Instruments. Magnetic Measurements. Dielectrics. Engineering Electronics. Electronic Instrumentation. Electrochemistry.

Optics and Metrology. Photometry and Colorimetry. Photographic Technology. Length. Engineering Metrology.

Heat. Temperature Physics. Thermodynamics. Cryogenic Physics. Rheology. Molecular Kinetics. Free Radicals Research.

Atomic and Radiation Physics. Spectroscopy. Radiometry. Mass Spectrometry. Solid State Physics. Electron Physics. Atomic Physics. Neutron Physics. Radiation Theory. Radioactivity. X-rays. High Energy Radiation. Nucleonic Instrumentation. Radiological Equipment.

Chemistry. Organic Coatings. Surface Chemistry. Organic Chemistry. Analytical Chemistry. Inorganic Chemistry. Electrodeposition. Molecular Structure and Properties of Gases. Physical Chemistry. Thermochemistry. Spectrochemistry. Pure Substances.

Mechanics. Sound. Mechanical Instruments. Fluid Mechanics. Engineering Mechanics. Mass and Scale. Capacity, Density, and Fluid Meters. Combustion Controls.

Organic and Fibrous Materials. Rubber. Textiles. Paper. Leather. Testing and Specifications. Polymer Structure. Plastics. Dental Research.

Metallurgy. Thermal Metallurgy. Chemical Metallurgy. Mechanical Metallurgy. Corrosion. Metal Physics.

Mineral Products. Engineering Ceramics. Glass. Refractories. Enameled Metals. Constitution and Microstructure.

Building Technology. Structural Engineering. Fire Protection. Air Conditioning, Heating, and Refrigeration. Floor, Roof, and Wall Coverings. Codes and Safety Standards. Heat Transfer. Concreting Materials.

Applied Mathematics. Numerical Analysis. Computation. Statistical Engineering. Mathematical Physics.

Data Processing Systems. SEAC Engineering Group. Components and Techniques. Digital Circuitry. Digital Systems. Analog Systems. Application Engineering.

- Office of Basic Instrumentation.
- Office of Weights and Measures.

BOULDER, COLORADO

Cryogenic Engineering. Cryogenic Equipment. Cryogenic Processes. Properties of Materials. Gas Liquefaction.

Radio Propagation Physics. Upper Atmosphere Research. Ionospheric Research. Regular Propagation Services. Sun-Earth Relationships. VHF Research. Radio Warning Services. Airglow and Aurora. Radio Astronomy and Arctic Propagation.

Radio Propagation Engineering. Data Reduction Instrumentation. Modulation Research. Radio Noise. Tropospheric Measurements. Tropospheric Analysis. Propagation Obstacles Engineering. Radio-Meteorology. Lower Atmosphere Physics.

Radio Standards. High Frequency Electrical Standards. Radio Broadcast Service. High Frequency Impedance Standards. Electronic Calibration Center. Microwave Physics. Microwave Circuit Standards.

Radio Communication and Systems. Low Frequency and Very Low Frequency Research. High Frequency and Very High Frequency Research. Ultra High Frequency and Super High Frequency Research. Modulation Research. Antenna Research. Navigation Systems. Systems Analysis. Field Operations.

NBS